Radiology Case Reports 19 (2024) 2633–2638

Available online at www.sciencedirect.com

ScienceDirect

journal homepage: www.elsevier.com/locate/radcr

Case Report

Atypical Gradenigo's syndrome in a pediatric case: A critical review of neuroimaging ☆

*Chae-Young Kim, MD, Min Young Lee, MD, PhD, Jae Yun Jung, MD, PhD, Ji Eun Choi, MD, PhD**

Department of Otolaryngology Head and Neck Surgery, Dankook University Hospital, College of Medicine, Dankook University, Cheonan, South Korea

ARTICLE INFO

Article history:
Received 3 January 2024
Revised 11 March 2024
Accepted 13 March 2024

Keywords:
Gradenigo's syndrome
Petrous apicitis
Pediatrics
Meckel's cave
Osteomyelitis
Petrositis

ABSTRACT

Gradenigo's syndrome, a rare but serious complication of otitis media, encompasses a triad of symptoms including otalgia, facial palsy, and abducens nerve palsy, pointing to the involvement of the petrous apex. This case report presents an 11-year-old boy with an atypical manifestation of Gradenigo's syndrome, characterized by the absence of classic features such as abducens nerve palsy and purulent otorrhea. MRI findings were significant for petrous apicitis extending to Meckel's cave and the cavernous sinus, along with abscess formation and clivus osteomyelitis. The report highlights the critical role of advanced neuroimaging, particularly MRI, in the diagnosis and management of this condition. It underscores the importance of recognizing atypical presentations of Gradenigo's syndrome and the effectiveness of imaging-guided conservative treatment strategies in pediatric otological cases.

Introduction

Gradenigo's syndrome, traditionally characterized by a triad of purulent otorrhea, trigeminal nerve pain, and abducens nerve palsy [1], is an uncommon but serious complication of otitis media and/or mastoiditis. In the modern antibiotic era, its classic presentation has become rare, with more subtle symptoms often observed [2]. This evolution underscores the importance of sophisticated imaging techniques, crucial for the accurate identification and management of Gradenigo's syndrome. This case report illustrates a radiologically diagnosed Gradenigo's syndrome, managed successfully with antibiotics.

Case report

An 11-year-old boy, previously diagnosed with COVID-19 a month earlier, visited the emergency department (ED) for ongoing left-sided headaches over the past 7 days. He also reported sharp, stabbing pain localized behind the left eye, without visual disturbances. He had a history of concurrent left

☆ Competing Interests: The authors declare that they have no known competing financial interests or personal relationships that could have appeared to influence the work reported in this paper.

* Corresponding author.
E-mail address: garimung@gmail.com (J.E. Choi).

https://doi.org/10.1016/j.radcr.2024.03.037

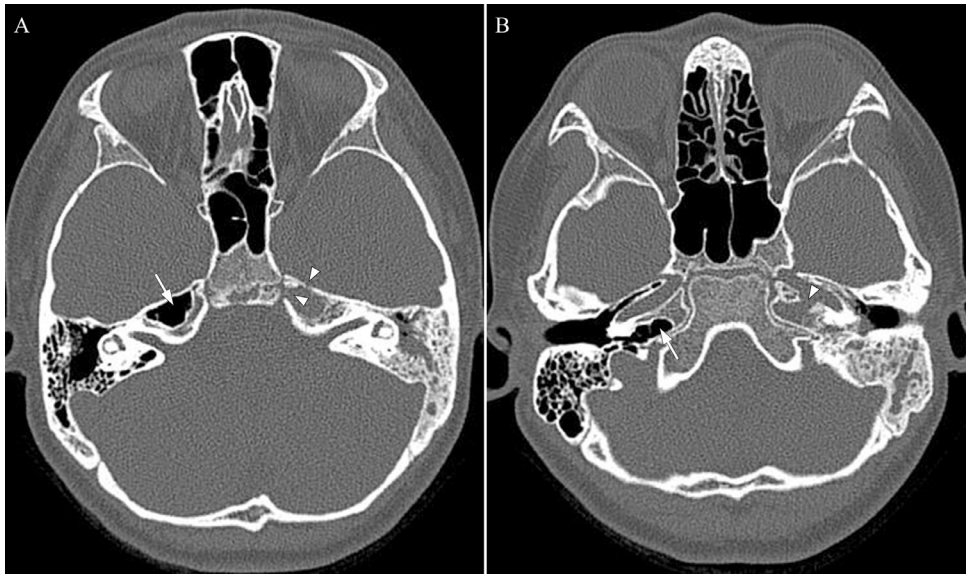

Fig. 1 – (A, B) Axial brain computed tomography (CT) images taken during the initial emergency department visit. The CT scan reveals diffuse soft tissue density within the left middle ear cavity (MEC), mastoid air cells (MACs), and petrous apex (PA), with a suspicious focal bone defect noted in the medial cortex of the left petrous apex (arrowheads). In contrast, the right petrous apex exhibits significant pneumatization at both anterior (arrow in A) and posterior (arrow in B) portion of the petrous apex.

ear pain. Upon examination, he was afebrile with normal vital signs. The Endoscopic ear examination showed a slightly bulging left tympanic membrane. Neurologic examination and the rest of the physical assessment were unremarkable. His white blood cell count was normal, but C-reactive protein was mildly elevated. A brain computed tomography (CT) revealed diffuse soft tissue density in left middle ear cavity, mastoid air cells, and petrous apex, with a suspicious focal bone defect in the left petrous apex (Figs. 1A and B). He was started on oral amoxicillin/clavulanate (Augmentin) and referred to the ear nose and throat (ENT) clinic for further evaluation, due to concerns of Gradenigo's syndrome.

Three days later, on the follow-up ENT visit, the boy still had headaches and eye pain despite the oral medication. Brain magnetic resonance imaging (MRI) revealed a fluid signal with heterogeneous enhancement extending from the left petrous apex to Meckel's cave (Figs. 2A-F). This was accompanied by a possible involvement of the left cavernous sinus (Fig. 2B), suggesting petrous apicitis. The heterogeneous enhancement, characterized by multiloculated rim enhancement rather than a solid rim, and the absence of diffusion restriction, indicates a complex inflammatory process that may represent varying stages of inflammation or abscess formation. The center of the lesion showed a low signal on diffusion-weighted imaging (DWI) and a high signal on apparent diffusion coefficient (ADC) imaging, which are consistent with either a mature abscess or parts of infective granulation tissue (Figs. 2E and F). Additionally, bone narrow enhancement in the left clivus suggested osteomyelitis (Figs. 2G and H). Magnetic resonance angiography (MRA) confirmed reduced flow in the distal portion of the left petrous internal carotid artery (IAC) (Fig. 2J). Ear endoscopy showed mild redness and slight bulging of the left tympanic membrane with a whitish effusion (Figs. 3A and B). Audiogram indicated mild conductive hearing loss in the left ear (Fig. 3C), and tympanometry yielded a type C tympanogram, suggesting impaired Eustachian tube function on the left (Fig. 3D). Ophthalmic evaluation confirmed normal visual acuity and ocular motility, but a grade 1 relative afferent pupillary defect (RAPD) was identified in the left eye. The optic disc appeared healthy.

One week after starting oral medication, the patient was admitted to the hospital and initiated on intravenous (IV) ceftriaxone and metronidazole. He showed marked improvement in headaches and eye pain within 48 hours of this treatment. Follow-up pupillary examinations indicated resolution of the previously observed grade 1 RAPD in the left eye. One week later, follow-up CT scans of the temporal bone showed improved aeration within the left middle ear cavity and mastoid air cells, indicative of reduced inflammation (Fig. 4A). Although persistent soft tissue density and a potential bone defect were noted in the left petrous apex seen on the CT (Fig. 4B), MRI with fat suppression (FS) demonstrated signs of improvement (Figs. 4C and D). T2-weighted imaging with FS (Fig. 4C) and contrast-enhanced T1-weighted imaging with FS (Fig. 4D) revealed a decreased in both size and extent of the rim-enhancing lesion in the left petrous apex, suggestive of a resolving abscess. Hyperintense signals in the bone marrow of the left clivus were seen on T2-weighted images with FS (Figs. 4E and G), while diminished enhancement, consistent with resolving inflammation, was noted on contrast-enhanced T1-weighted images with FS (Figs. 4F and H). However, a persistently narrow diameter of the left distal ICA petrous segment with thin enhancement was still present (Fig. 4D). Ear endoscopy showed the left tympanic

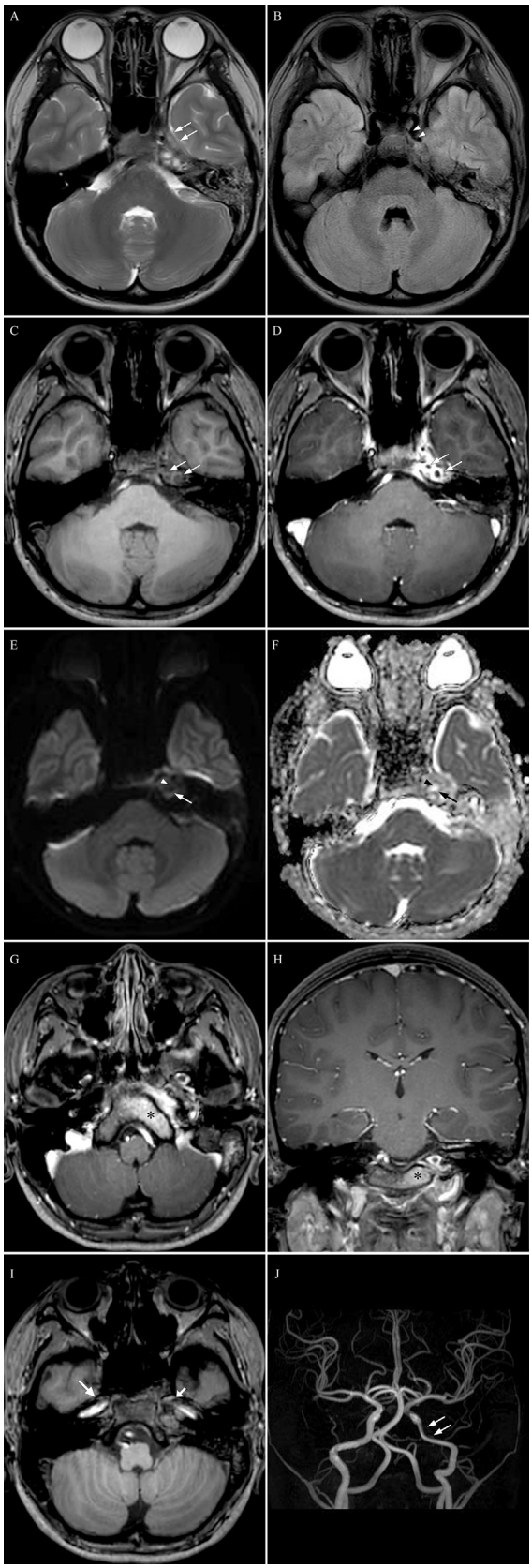

membrane had returned to normal. The patient was discharged following a two-week course of IV antibiotics (ceftriaxone for 2 weeks and metronidazole for 1 week) and transitioned to a 1-week course of oral amoxicillin/clavulanate (Augmentin). Three weeks post-discharge, he continued to improve, and antibiotics were discontinued. Three months later, the final MRI scan showed resolution of signal abnormality in the left petrous apex, with a normalized diameter of distal ICA petrous segment (Fig. 5). At the seven-month outpatient follow-up, the patient remained well with no signs of recurrence.

Discussion

In this case of an 11-year-old boy diagnosed with petrous apicitis, presenting with abscess formation and osteomyelitis of the clivus, the role of advanced neuroimaging is paramount. Petrous apicitis, a rare complication of otitis media, poses diagnostic challenges due to the complex anatomy of the petrous apex. This area, nestled between the inner ear and clivus, is adjacent to critical structures like the cavernous sinus, Dorello canal, and Meckel's cave, necessitating precise imaging for accurate diagnosis and treatment planning.

Fig. 2 – (A-F) Brain magnetic resonance imaging (MRI) and magnetic resonance angiography (MRA) obtained prior to admission. (A) Axial T2-weighted image reveals extensive hyperintense fluid collection throughout the left petrous apex (asterisk), extending to Meckel's cave (arrows). (B) The axial fluid-attenuated inversion recovery (FLAIR) MRI indicates a hyperintense signal and potential expansion toward the left cavernous sinus (arrowhead). (C) An axial T1-weighted image without contrast highlights a hypointense center with an isointense rim in the left petrous apex (arrows), reaching into Meckel's cave. (D) A contrast-enhanced T1-weighted image reveals multiloculated rim enhancement around the hypointense fluid (arrows), which could represent varying stages of inflammation and/or abscess formation. (E) Diffusion weighted imaging (DWI; b=1000) exhibits a high signal at the rim-enhancing portions of the lesion (arrow) and (F) apparent diffusion coefficient (ADC) imaging shows a low signal at these same rim-enhancing portions (arrow), suggesting active inflammation or abscess formation. Conversely, the non-enhancing center of the lesion exhibits a low signal on DWI (arrowhead in E) and a high signal on ADC (arrowhead in F), consistent with the features of mature abscess or parts of infective granulation tissue. Axial (G) and coronal (H) T1-weighted image with contrast enhancement depict ill-defined enhancement in the bone marrow of the left clivus (asterisk). (I) An axial T1-weighted image illustrates diminished flow signal intensity within the left petrous internal carotid artery (ICA, short arrow), in contrast to the normal right petrous IAC (long arrow). (J) MRA also shows smooth narrowing in the distal portion of left petrous ICA (arrows).

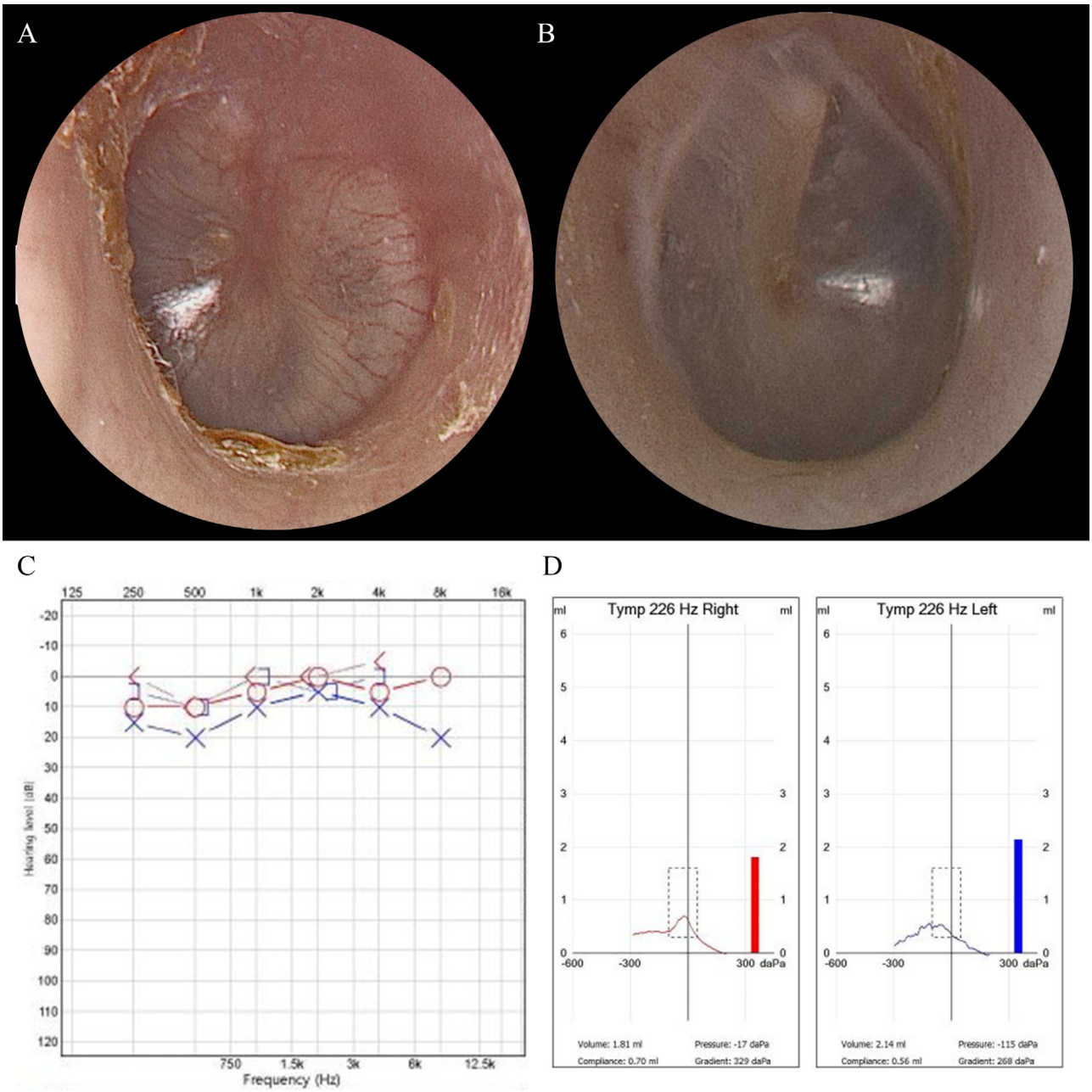

Fig. 3 – Otologic evaluation performed prior to admission. (A) Ear endoscopy reveals mild redness and slight bulging in the posterior quadrants of the left tympanic membrane. (B) The right tympanic membrane appears normal. (C) Pure tone audiometry indicates a normal right audiometric threshold (red in C) and mild left conductive hearing loss with an air–bone gap of 10 dB HL (blue in C). (D) Tympanometry results in a type A tympanogram for the right ear, which is normal, and type C for the left ear, indicating decreased Eustachian tube function.

CT is considered the first choice in a patient suspected of having a petrous apex lesion, because it has a high sensitivity for detection of changes in bone structures. The most common finding on CT scan is opacification or coalescence of the air cells in the petrous apex, accompanied by erosive lysis with ill-defined irregular margins of its bony structure. Radiological studies have shown that a significant percentage of children display petrous apex pneumatization with communicating tracts to the middle ear [3], providing pathways for infection spread. In this case, CT imaging of the well-pneumatized petrous apex displayed typical petrous apicitis findings (Fig. 1), confirming the diagnosis and demonstrating the infection's spread from the middle ear to the petrous apex.

MRI complements CT by offering superior visualization of soft tissues in petrous apicitis, typically presenting with low signal intensity on T1, high signal intensity on T2, and con-

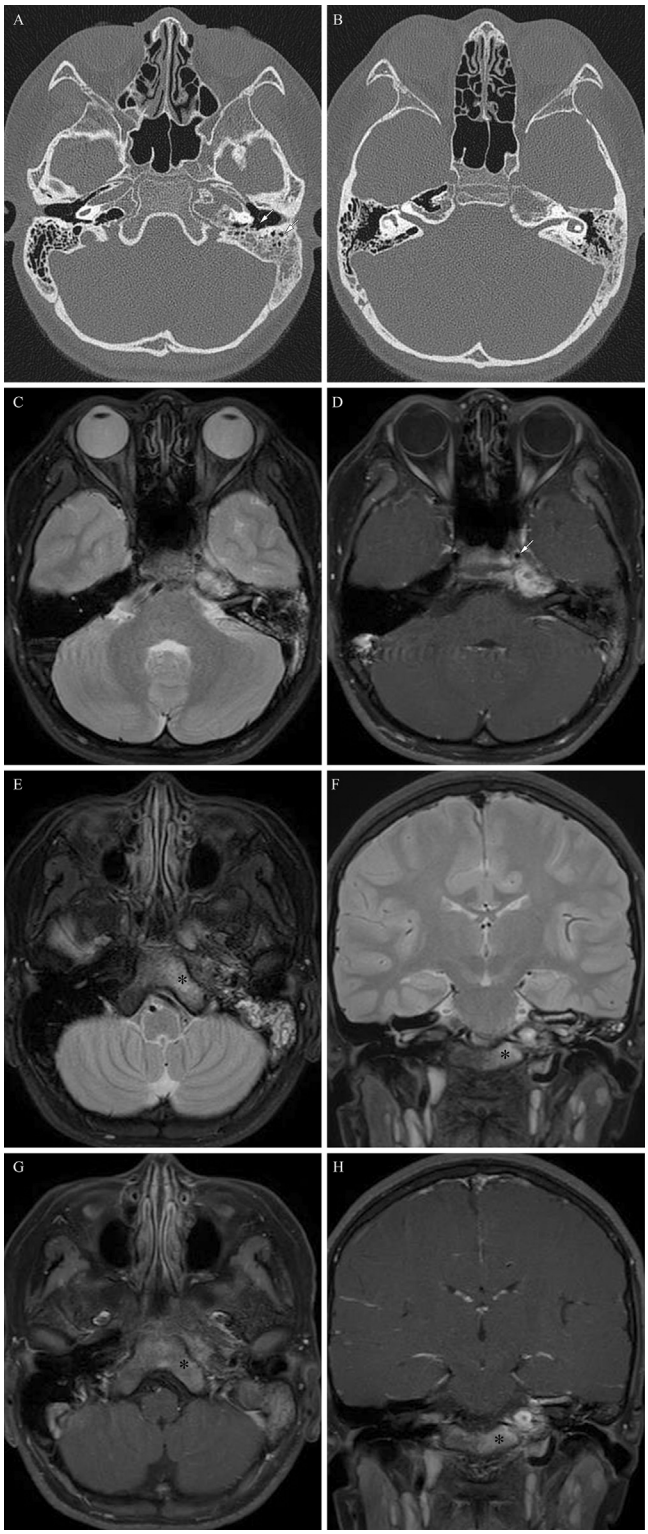

trast enhancement within the petrous apex. Thickening of Meckel's cave and cavernous sinus dura, along with signs of cavernous sinus thrombosis, are critical to assess. In this case, MRI showed fluid signal extension from the left petrous apex to Meckel's cave with peripheral enhancement (Fig. 2A), suggesting trigeminal nerve irritation, correlating with the patient's retro-bulbar pain. DWI has proven crucial for early diagnosis, offering high sensitivity and specificity for differentiating abscesses from other inflammatory or neoplastic pathologies. Notably, a contrast-enhanced MRI incorporating DWI typically identifies an abscess as a multiloculated rim enhancement lesion with diffusion restriction, marked by hyperintense signals on DWI and corresponding hypointense signals on ADC imaging. However, the non-enhancing center exhibited a low signal on DWI and a high signal on ADC, consistent with a mature abscess or parts of infective granulation tissue, lacking the typical diffusion restriction observed in the center of most abscesses (Figs. 2E and F). This pattern suggests the presence of a complex inflammatory process, possibly indicative of multiple stages of inflammation and healing [4]. In cases of osteomyelitis involving adjacent bony structures like the clivus or sphenoid bone, lesions appear hypointense on T1, distinct from normal bone marrow's high signal. Hyperintensity on T2-weighted images and contrast enhancement also typically indicate osteomyelitis. As evidence in this case (Figs. 4C-H), FS techniques are invaluable in highlighting bone marrow lesions and differentiating hyperemic inflammatory tissue from abscess formation. When infection reaches cortical margins of the carotid canal, MRA effectively visualizes reduced blood flow. This case's MRA revealed decreased flow in the distal portion of the left petrous ICA (Fig. 2J), potentially due to ICA vasospasm or arteritis. Such reduced blood flow could have impacted the optic nerve, explaining the transient grade 1 RAPD observed in the patient.

Fig. 4 – (A-G) Follow-up CT and MRI obtained one week after hospital admission. (A) Axial CT of the temporal bone reveals improved aeration within the left middle ear cavity and mastoid air cells (thin arrows), suggesting a diminished inflammatory process. (B) The CT, however, shows consistent soft tissue density in the left petrous apex, with a focal bone defect still visible in the medial cortex. (C) An axial T2-wighted MRI with fat suppression (FS) demonstrates a reduced lesion size in the left petrous apex, with a less prominent extension than earlier images. (D) Post-contrast T1-weighted MRI with FS shows a decreased rim-enhancing lesion within the left petrous apex, indicative of reduced inflammation. However, a slightly narrowed left distal ICA within the petrous segment with thin enhancement along the carotid canal persists (arrow). (E-F) Axial (E) and coronal (F) T2-weighted MRIs with FS reveal hyperintense signals in the bone marrow of the left clivus (asterisk). (G-H) Axial (G) and coronal (H) contrast-enhanced T1-weighted MRIs with FS show reduced enhancement in the left clivus, suggesting a subsiding inflammatory process (asterisk).

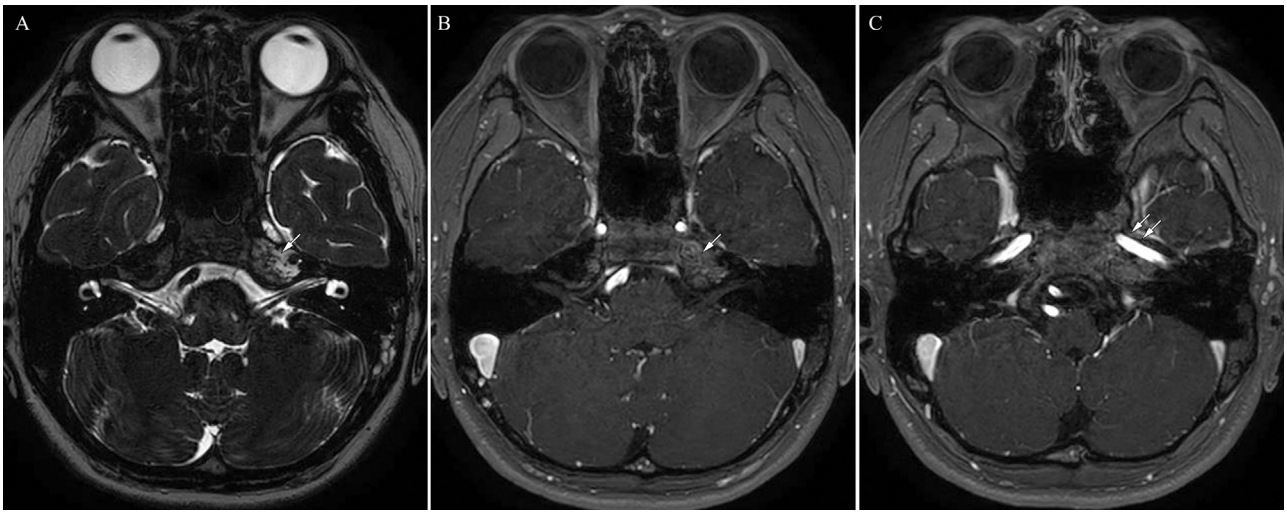

Fig. 5 – (A-C) Internal acoustic canal (IAC) MRI obtained during a three-month follow-up outpatient visit. (A) Volume Isotropic Turbo spin echo Acquisition (VISTA) MRI sequence presents continuous high T2 signal intensity in the left petrous apex (arrow), consistent with residual inflammation or post-inflammatory changes. (B) Contrast-enhanced T1 MRI sequence shows subtle enhancement in the same region (arrow), which is indicative of post-inflammatory granulation tissue rather than ongoing active inflammation. (C) A T1-weighted post-contrast MRI depicts the normalized diameter of the left distal ICA petrous segment (arrows), signifying the resolution of the previous vascular narrowing.

The traditional surgical approach for Gradenigo syndrome has evolved towards conservative management with IV antibiotics, aided by these advanced imaging techniques. Broad-spectrum antibiotics, including ceftriaxone, cefotaxime, imipenem, or piperacillin/tazobactam, are initially recommended. IV antibiotics are recommended for at least 2-3 weeks. Patients with an associated osteomyelitis may require up to 6 weeks of antibiotics. The inclusion of metronidazole covers potential anaerobic organisms, a prudent choice in abscess cases [5]. This case report demonstrates successful treatment through medical management, showcasing the pivotal role of modern imaging and antibiotic therapy in managing complex cases of petrous apicitis.

Conclusion

This case highlights the complexity of Gradenigo's syndrome in the modern medical era and underscores the importance of a timely, accurate diagnosis through advanced imaging techniques. This approach, coupled with appropriate antibiotic therapy, significantly reduced the potential morbidity and mortality associated with the condition. Our findings emphasize the necessity of integrating clinical and imaging data to achieve optimal patient outcomes in complex cases like Gradenigo's syndrome.

Patient consent

All patient data was anonymized, and informed consent was obtained from the patient's parents for scientific work and publication.

REFERENCES

[1] Gradenigo G. Über die paralyse des nervus abducens bei otitis. Archiv für Ohrenheilkunde 1907;74(1):149–87.
[2] McLaren J, Cohen MS, El Saleeby CM. How well do we know Gradenigo? A comprehensive literature review and proposal for novel diagnostic categories of Gradenigo's syndrome. Int J Pediatr Otorhinolaryngol 2020;132:109942. doi:10.1016/j.ijporl.2020.109942.
[3] Hardcastle T, McKay-Davies I, Neeff M. Petrous apex pneumatisation in children: a radiological study. J Laryngol Otol 2020;24:1–6. doi:10.1017/S0022215120001681.
[4] Kim JH, Park SP, Moon BG, Kim DR. Brain abscess showing a lack of restricted diffusion and successfully treated with linezolid. Brain Tumor Res Treat 2018;6(2):92–6. doi:10.14791/btrt.2018.6.e16.
[5] Jacobsen CL, Bruhn MA, Yavarian Y, Gaihede ML. Mastoiditis and Gradenigo's syndrome with anaerobic bacteria. BMC Ear Nose Throat Disord 2012;12:10. doi:10.1186/1472-6815-12-10.